Chemosphere 214 (2019) 239–249

Contents lists available at ScienceDirect

Chemosphere

journal homepage: www.elsevier.com/locate/chemosphere

Formation of lead ferrites for immobilizing hazardous lead into iron-rich ceramic matrix

Xingwen Lu [a, b, d], Jiani Yang [a], Xun-an Ning [a], Kaimin Shih [b], Fei Wang [c, b, *], Yuanqing Chao [e, d]

[a] School of Environmental Science and Engineering, and Institute of Environmental Health and Pollution Control, Guangdong University of Technology, Guangzhou 510006, China
[b] Department of Civil Engineering, The University of Hong Kong, Pokfulam Road, Hong Kong, China
[c] School of Environment, Guangzhou Key Laboratory of Environmental Exposure and Health, and Guangdong Key Laboratory of Environmental Pollution and Health, Jinan University, Guangzhou 510632, China
[d] Guangdong Provincial Key Laboratory of Environmental Pollution Control and Remediation Technology, Sun Yat-sen University, Guangzhou, 510275, China
[e] School of Environmental Science and Engineering, Sun Yat-sen University, Guangzhou, 510275, China

HIGHLIGHTS

- Lead was incorporated to lead ferrites (i.e. δ-, γ- and β-phase) by hematite.
- Crystal structure transformation between δ-, γ- and β- phase was detected.
- δ-, γ- and β-phase dominantly formed at Pb/Fe of 1/(1–3), 1/(4–7) and 1/(7–12).
- Incongruent dissolution of δ-, γ- and β-phase in leaching test was observed.

ARTICLE INFO

Article history:
Received 10 July 2018
Received in revised form
14 September 2018
Accepted 19 September 2018
Available online 20 September 2018

Handling Editor: Xiangru Zhang

Keywords:
Lead
Stabilization
Lead ferrite
Mechanism
Crystal transformation

ABSTRACT

A strategy of immobilizing lead in the framework of ferrite-ceramic matrix, to reduce its environmental hazard was explored in this study. The mechanisms of incorporating lead into lead ferrites (δ-phase ($2PbO \cdot Fe_2O_3$), γ-phase ($PbO \cdot (2–2.5)Fe_2O_3$) and β-phase ($PbO \cdot (5–6)Fe_2O_3$)) was revealed by observing the phase transformation in the products. The δ-phase was dominantly formed at low temperature of 700–800 °C at Pb/Fe of 1/1-1/3. The significant growth of γ-phase was observed at 750–850 °C and Pb/Fe of 1/4-1/7. The β-phase substantially formed at 900–1000 °C with Pb/Fe of 1/7-1/12. The transformation of δ-phase to γ-phase and/or β-phase indicated the destruction of δ-phase unit and reconstruction of γ-phase and β-phase units during sintering process. However, the transformation of γ-phase into β-phase suggested a structure conversion process, local structural changes arose as a consequence of the addition of Fe_2O_3. When comparing the leaching ability of δ-, γ- and β-phase, the results showed the superiority of β-phase for lead immobilization over the longer leaching period.

1. Introduction

Lead (Pb) is a metal widely used for various technical purposes due to its versatile physical and chemical properties. Thus, lead-containing wastes increases constantly in the manufacturing of lead batteries and oil-based paints, mining, plating, electronics and wood production (Conrad and Hansen, 2007; Venäläunen, 2011). The release of lead into the environment from its manufacturing industries is of serious environmental concern. Since lead is highly toxic and a non-biodegradable metal that tends to accumulate in the cells of living organisms, which causes severe damage to the kidneys, liver, and the nervous and reproductive systems of humans (Gupta et al., 2011). Therefore, remediation of the lead-containing wastes has become more and more important in recent years owing to the reinforcement in the environmental protection.

* Corresponding author. School of Environment, Guangzhou Key Laboratory of Environmental Exposure and Health, and Guangdong Key Laboratory of Environmental Pollution and Health, Jinan University, Guangzhou 510632, China.
E-mail address: wf1984@jnu.edu.cn (F. Wang).

https://doi.org/10.1016/j.chemosphere.2018.09.121
0045-6535/

Ceramic technologies are considered to be the versatile for rendering hazardous waste inert because they immobilize hazardous metals in a stable crystallization phase to reduce the hazardous metal leachability in waste materials (Xu et al., 2008, 2009). The immobilization mechanism is strongly dependent on phase transformation and evolution of heavy metals during the sintering process (Li et al., 2017; Li et al., 2011a,b; Hu et al., 2010) In addition, the leaching behaviors of heavy metals from the ceramic matrix are determined by the crystal structure of the metal-hosting phases (Hsieh et al., 2013; Lu et al., 2008). Besides aluminium and silica oxide, a commonly used material in ceramic processing is hematite (α-Fe_2O_3), which behaves as a refractory antiflux material in combination with alkalis. Owing to its relatively low cost and wide availability, hematite is known as a feasible matrix for the immobilization of various hazardous metals in waste, and shown effective stabilization ability (Mao et al., 2014; Li et al., 2011a,b; Shih et al., 2006). By sintering with hematite precursor, the hazardous Ni, Cu, Zn and Cd can be fairly fixed into ferrite spinal structures, and the hazardous metal leachability was significantly reduced (Shih et al., 2006; Su et al., 2017, 2018; Li et al., 2017). However, potential reactions between lead and hematite may strongly influence the leachability of hazardous metals from the matrix. To create a successful lead stabilization technology, a comprehensive understanding of the mechanisms for transforming lead into ferrite-ceramic matrix is crucial.

Because the composition of metals in waste streams can fluctuate and it would cause the varied stoichiometric values of Pb/Fe for ferrite synthesis. Furthermore, the relative incorporation of Pb and Fe was reported depends critically on the initial Pb/Fe molar ratio (Sahu et al., 2012; Diop et al., 2010). Previous studies have identified 11 ferrite complexes in PbO-Fe_2O_3 system, i.e., $8PbO\cdot Fe_2O_3$, $3PbO\cdot Fe_2O_3$, $2PbO\cdot Fe_2O_3$, $3PbO\cdot 2Fe_2O_3$, $PbO\cdot Fe_2O_3$, $PbO\cdot 2Fe_2O_3$, $2PbO\cdot 5Fe_2O_3$, $PbO\cdot 3Fe_2O_3$, $PbO\cdot 4Fe_2O_3$, $PbO\cdot 5Fe_2O_3$ and $PbO\cdot 6Fe_2O_3$ (Sahu et al., 2012; Diop et al., 2010; Rivolier et al., 1993; Raghavan, 1989). These ferrite complexes with different initial stoichiometric ratios were considered as the potential lead ferrites in sintered PbO/Fe_2O_3 products (Sahu et al., 2012, 2013; Diop et al., 2010). Among these complexes, δ-phase ($2PbO\cdot Fe_2O_3$), γ-phase ($PbO\cdot(2-2.5)Fe_2O_3$) and β-phase ($PbO\cdot(5-6)Fe_2O_3$) were determined to be stable phases (Sahu et al., 2012, 2013; Diop et al., 2010). Although the formation of lead ferrites from a PbO-Fe_2O_3 system is feasible, the reaction sequences involved in the incorporation of lead under different thermal conditions with various Pb/Fe molar ratios has remained unclear. To determine the potential mechanistic processes of lead incorporation, it is essential to identify the structures of crystalline phases in ceramic products. Furthermore, the robustness of the product(s) to acids should be examined with leaching tests to verify the metal stabilization effects. It has been demonstrated that constant-pH leaching test is a useful tool to assess the leachability of products, because CPLT could maintain the pH in a steady level (Al-Abed et al., 2007; Islam et al., 2004; Jackson et al., 1984). In TCLP leaching test, the decomposition of metal-containing crystal framework and cation exchange with solution protons may lead to the significant increase of leachate pH (Shih et al., 2006; Tang et al., 2011; Lu et al., 2013). However, the pH in constant-pH leaching experiments leachability can maintain stable. Thus, the leachability of different metal structures can be compared in the same condition.

The objective of this work is to in-depth study the lead stabilization mechanisms with hematite. The XRD technique was used to identify the structures of crystalline phases, and the metal incorporation mechanisms were further analyzed based on the XRD results. At the end of the study, the constant-pH leaching tests were carried out to evaluate the intrinsic phase durability and metal leachability in sintered products.

2. Materials and methods

2.1. Materials

PbO is common forms in the sewage sludge after thermal processes (Udayanga et al., 2018), in this study PbO (Sigma-Aldrich) was used as the lead source, representing its major form in the thermally treated lead-laden sludge. The PbO powder was identified by X-ray diffraction (XRD) assisted with the Powder Diffraction File (PDF) database published by International Centre for Diffraction Data (ICDD) as a mixture of the litharge (α-PbO; ICDD PDF #77–1971) and massicot (β-PbO; ICDD PDF #05–0561) phases. Hematite powder was purchased from Sigma-Aldrich, and its XRD pattern matched that of standard hematite peaks (ICDD PDF #78–1996). The PbO and Fe_2O_3 powders were calcined in air at 300 °C for 3 h to remove the moisture content before use.

2.2. Thermal reaction

To evaluate the feasibility of Pb incorporation, hematite precursor and PbO were mixed by ball milling in water slurry with Pb/Fe molar ratios of 1/1, 1/4 and 1/12 for 18 h. The ball milling was conducted in a planetary ball mill consisting of four tungsten carbide grinding jars (100 ml each) at a rotation speed of 500 rpm. Sequentially, the mixtures were dried at 105 °C for 48 h in a vacuum oven, and then further homogenized by extended mortar grinding for 10 min in an agate mortar. Before thermal treatment, the derived powder was pressed into 20-mm pellets at 650 MPa to ensure consistent compaction of the powder for the sintering process. For the incorporation reaction, a well-control thermal treatment scheme at the targeted temperature was applied. In most cases, the dwell time was fixed at 3 h for sintering temperatures ranging from 600 °C to 1050 °C.

2.3. X-ray diffraction

After sintering, the samples were ground using an agate mortar and pestle to a particle size of no more than 10 μm for XRD analysis. The powder XRD patterns were recorded on a Bruker D8 Advance X-ray powder diffractometer equipped with Cu Kα radiation and a LynxEye detector. The diffractometer was operated at 40 kV and 40 mA, and the 2θ scan range was from 10° to 80°, with a step size of 0.02° and a scan speed of 0.3 s per step. Phase identification was performed with the Eva XRD Pattern Processing software (Bruker, Germany) by matching the powder XRD patterns with those retrieved from the standard powder diffraction database published by the ICDD.

2.4. Leaching tests

The potential leaching ability of lead-bearing products were compared by constant-pH leaching experiments. The target product powder (<45 μm) was subjected to batch leaching test in the plastic vessels at a liquid/solid ratio of 50 L/kg (4 g products powder and 200 ml pH 5.0 acetic acid solution) and a total equilibration time of 168 h. Acid (1 N HNO_3) was added into plastic vessels to maintain the pH constant at 5.0 by a pH stat system. The continuously stirring was conducted to keep the mixture homogeneous and the leaching vessel was maintained at room temperature (23 ± 0.5 °C). At different record times, the suspensions were allowed to settle for 5 min and small aliquots of 5 ml of the upper liquid were taken and centrifuged. Another 5 ml pH 5.0 acetic acid solution together with the filtered solids was added to the vessels. At the end of each agitation period, the leachates were filtrated using 0.2 μm syringe filters. The total concentrations of Pb and Fe

were analytically determined by inductively coupled plasma - atomic emission spectroscopy (ICP-AES; Perkin-Elmer Optima 3300 DV, Norwalk, CT, USA).

3. Results and discussion

3.1. Effect of temperature on phase transformation in Pb/Fe of 1/1 system

Although previous studies have considered 11 ferrite complexes with different initial stoichiometric ratios as the potential lead ferrites in PbO/Fe_2O_3 system (Sahu et al., 2012, 2013; Diop et al., 2010). Only complexes of δ-phase ($2PbO{\cdot}Fe_2O_3$), γ-phase ($PbO{\cdot}(2–2.5)Fe_2O_3$) and β-phase ($PbO{\cdot}(5–6)Fe_2O_3$)) were determined to be stable phases (Sahu et al., 2012, 2013; Diop et al., 2010). As intermediate phases was thermally unstable in the treatment process, Pb/Fe molar ratios of 1/1, 1/4, and 1/12 were used to study the effects of temperature. Firstly, samples with Pb/Fe molar ratio of 1/1 in PbO/Fe_2O_3 system were sintered at 600–1000 °C and XRD patterns of the products were shown in Fig. 1. At temperatures above 700 °C, no signals from PbO or Fe_2O_3 were found in Pb/Fe molar ratio of 1/1 system. At 750–850 °C, δ-phase was found to be the only lead-containing crystalline phase in sintered products. The transformation of lead into δ-phase ($2PbO{\cdot}Fe_2O_3$) can be described by Equation (1),

$$2\ PbO_{(s)} + Fe_2O_{3(s)} \rightarrow \delta\text{-phase}(2PbO{\cdot}Fe_2O_3)_{(s)} \quad (1)$$

However, with a further increase of the temperature to 900 °C, the reduction of δ-phase indicated that this compound may be only thermally stable at temperatures below 900 °C. When temperatures increased from 900 to 1000 °C, the decrease of δ-phase and the increase of γ-phase and β-phase indicating the transformation of δ-phase into γ-phase and β-phase. At 1000 °C, the complete decomposition of δ-phase and the significant crystal growth of β-phase were detected.

The powder diffraction database shows that the strongest diffraction peak reflected from the (2 0 4) plane of δ-phase was located at $2\theta = 32.41°$. Thus, the 2θ range of 32.0–32.8° demonstrated the details in phase growth and reduction of δ-phase. Fig. 1 (b) illustrated that the peak intensity of δ-phase increased with an increase in sintering temperature before reaching its maximum at 850 °C, and followed by a decrease in intensity when temperature further increased from 850 to 950 °C. Further growth of β-phase can be carried out by observing its major peak located at $2\theta = 36.10°$, which correspond to the (0 0 8) plane of its structure (Fig. 1 (c)). Starting from 900 °C, the initiation of crystalline β-phase formation was observed. A higher temperature resulted in an increase in peak intensity, which indicates a continuing growth of the δ-phase phase from 900 to 1000 °C. The significant growth of β-phase was clearly observed at 1000 °C.

3.2. Effect of temperature on phase transformation in Pb/Fe of 1/4 system

In Pb/Fe of 1/4 system, γ-phase ($PbO{\cdot}(2–2.5)Fe_2O_3$) was the only stable phase of product reported in equilibrium experiments (Sahu et al., 2012, 2013; Diop et al., 2010). However, three stages of phase transformation were observed in Fig. 2(a) for the system with a Pb/Fe ratio of 1/4, representing different lead incorporation behaviors at the corresponding temperatures. Firstly, at 700 °C, the reaction of PbO and Fe_2O_3 in a non-equilibrium system resulted in the formation of δ-phase, possibly facilitated by the much higher standard Gibbs energy for the formation of δ-phase than γ-phase (Sahu et al., 2012) in this system. In the second stage, the reduction of δ-phase and increase of γ-phase were observed at 700–850 °C.

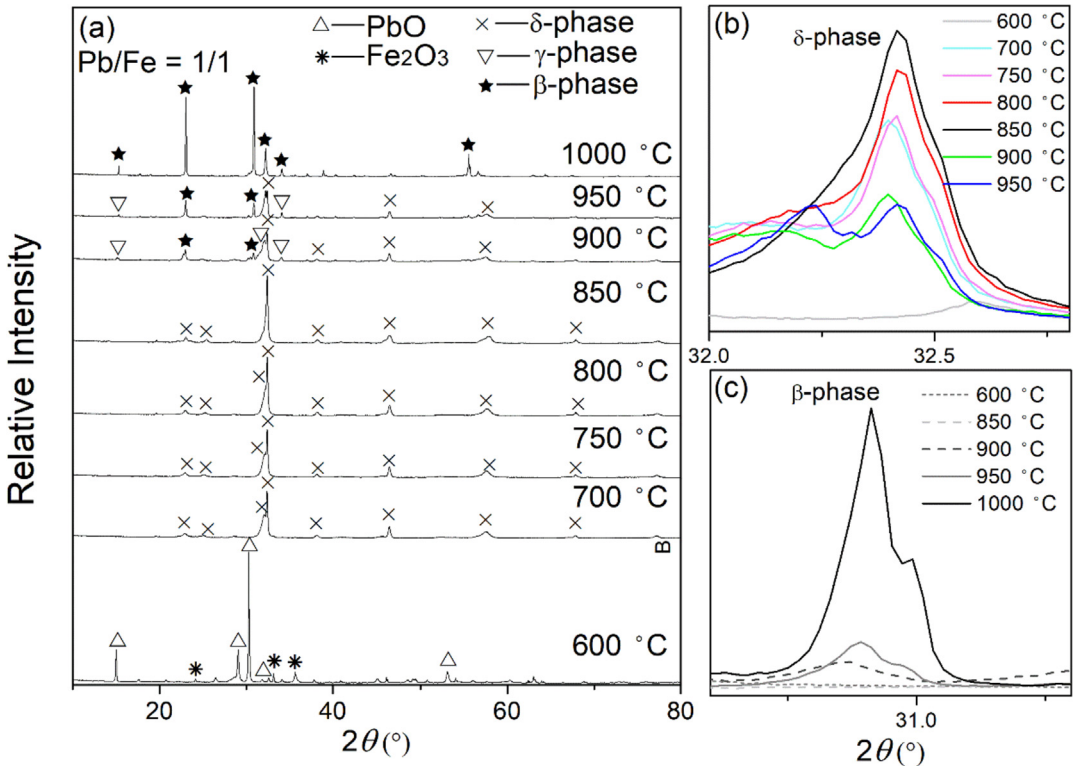

Fig. 1. XRD patterns for (a) $2\theta = 10–80°$, (b) $2\theta = 32.0–32.8°$ and (c) $2\theta = 30.6–31.3°$ of Pb/Fe molar ratio of 1/1 system. The result show the formation of δ-phase ($2PbO{\cdot}Fe_2O_3$, PDF # 34–0871), γ-phase ($PbO{\cdot}(2–2.5)Fe_2O_3$, PDF # 49–0753) and β-phase ($PbO{\cdot}(5–6)Fe_2O_3$, PDF #41–1373) when sintering PbO/Fe_2O_3 at 600–1000 °C for 3 h.

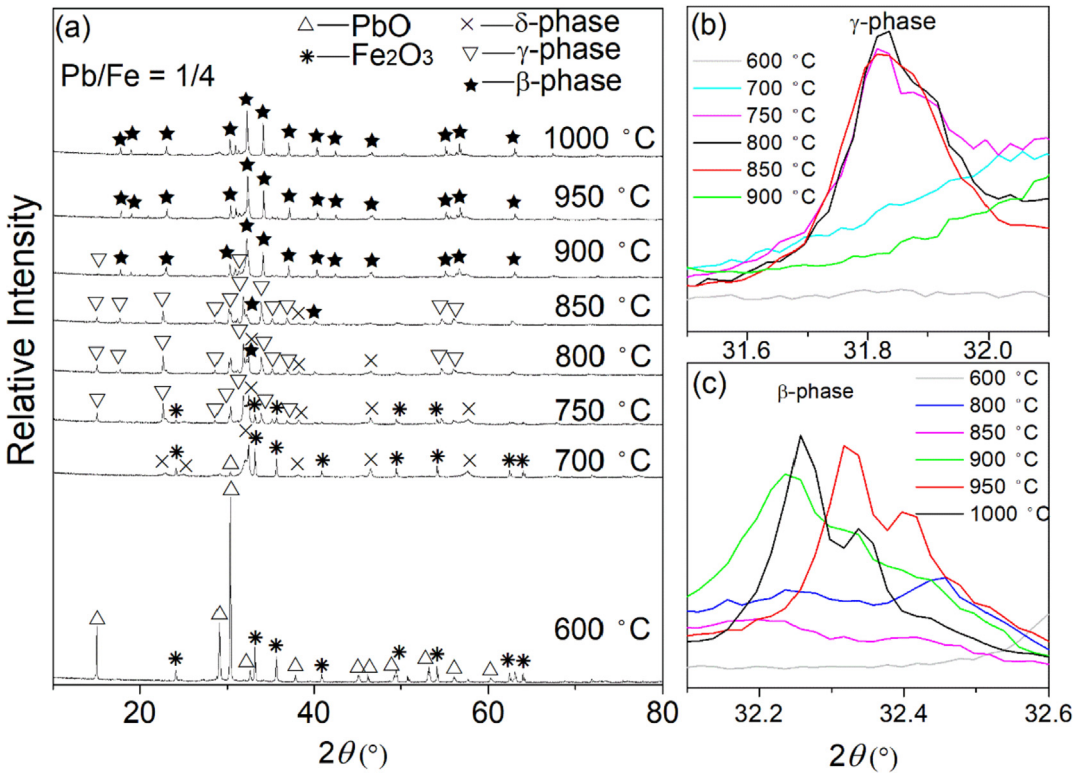

Fig. 2. (a) $2\theta = 10–80°$, (b) $2\theta = 31.5–32.1°$ and (c) $2\theta = 32.1–32.6°$ of Pb/Fe molar ratio of 1/4 system. The result show the changes of peak intensity of δ-, γ- and β-phase in the products sintered at 600–1000 °C for 3 h.

As the decomposition temperature of δ-phase was found at ~900 °C, this result may suggest that the solid-state reaction of δ-phase with Fe_2O_3 lead to the formation of γ-phase at 750–850 °C. Thus, the formation mechanisms of γ-phase can be represented as follows:

$$\delta\text{-phase}(2PbO\cdot Fe_2O_3)_{(s)} + (3–4)Fe_2O_{3(s)} \rightarrow 2\gamma\text{-phase}(PbO\cdot(2–2.5)Fe_2O_3)_{(s)} \quad (2)$$

$$PbO_{(s)} + (2–2.5)Fe_2O_{3(s)} \rightarrow \gamma\text{-phase}(PbO\cdot(2–2.5)Fe_2O_3)_{(s)} \quad (3)$$

Finally, the phase signal of γ-phase decreased dramatically due to the decomposition of γ-phase at ~880 °C (Nevriva and Fischer, 1986). However, the significant increase of β-phase was observed at 850–900 °C, which indicated the transformation of γ-phase into β-phase as the temperature increase. The β-phase become the only crystalline Pb-hosting phase at 950–1000 °C.

The formation of the γ-phase is demonstrated by the increase of the strongest peak located at $2\theta = 31.82°$, which is attributed to the (3 1 3) diffraction plane (Fig. 2 (b)). The increase of the diffraction peak illustrated the effective formation of γ-phase starting at 750 °C and reached its maximum at 800 °C. With further increase of the sintering temperatures, the reduction of γ-phase was observed and its peak intensity dramatically decreased at 900 °C. Further growth details of the β-phase can be observed by its highest peak located at $2\theta = 32.28°$ which correspond to the (1 0 7) plane of its structure (Fig. 2 (c)). The initiation of poor crystalline β-phase was found at 800 °C, whereas, significant crystal growth of β-phase was observed at 900 °C and the peak intensity of β-phase was quite stable even the temperature increased to 1000 °C.

3.3. Effect of temperature on phase transformation in Pb/Fe of 1/12 system

The XRD patterns of sintering products with a Pb/Fe ratio of 1/12 in PbO/Fe_2O_3 system was shown in Fig. 3. The β-phase is the only product phase reported in $PbO\text{-}Fe_2O_3$ equilibrium system with Pb/Fe molar ratio of 1/12 (Diop et al., 2010; Nevřiva and Fischer, 1986). However, δ-phase firstly appeared as the product phase at lower temperature of 700 °C at this system. As the standard enthalpy of the formation of δ-phase was found to be much higher than that of β-phase (Sahu et al., 2013), it can be concluded that the reaction between PbO and Fe_2O_3 energetically favors the formation of δ-phase over that of β-phase. The peak intensity of δ-phase quickly dropped when the temperature was increased to 750 °C, and followed by the appearance of γ-phase and β-phase. As the reported decomposition temperature (~880 °C) (Diop et al., 2010; Nevřiva and Fischer, 1986) of δ-phase is higher than 750 °C, the formation of γ-phase and β-phase was occurred in the solid-state reaction between δ-phase and Fe_2O_3 in this Fe-rich system. With further increase of temperature, a gradual decrease of γ-phase was observed at 750–850 °C. As the decomposition temperature of γ-phase was reported at ~880 °C (Nevřiva and Fischer, 1986), γ-phase may react with Fe_2O_3 for the formation of β-phase other than decomposition. The significant formation of β-phase was observed at 850 °C. And the formation of β-phase can be described by the following equations:

$$\delta\text{-phase}(2PbO\cdot Fe_2O_3)_{(s)} + (9–11)Fe_2O_{3(s)} \rightarrow 2\beta\text{-phase}\ (PbO\cdot(5–6)Fe_2O_3)_{(s)} \quad (4)$$

$$\gamma\text{-phase}(PbO\cdot(2–2.5)Fe_2O_3)_{(s)} + (2.5–4)Fe_2O_{3(s)} \rightarrow \beta\text{-phase}\ (PbO\cdot(5–6)Fe_2O_3)_{(s)} \quad (5)$$

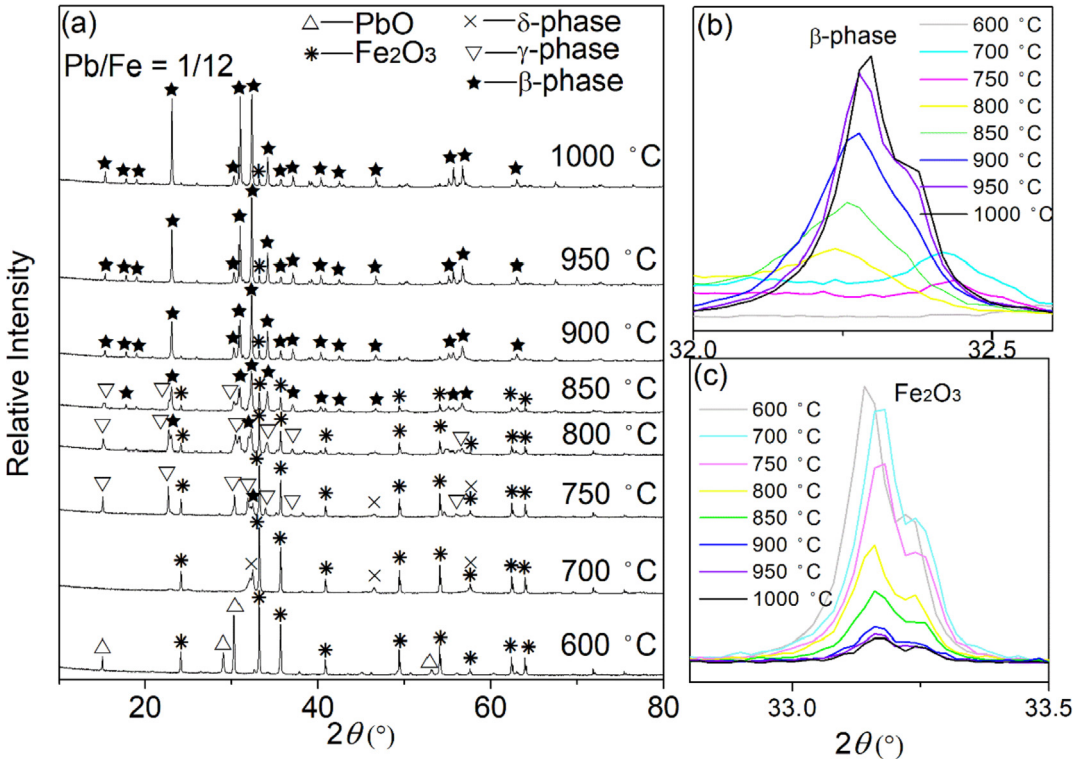

Fig. 3. XRD patterns for (a) $2\theta = 10–80°$, (b) $2\theta = 32.0–32.6°$ and (c) $2\theta = 32.8–33.5°$ of Pb/Fe molar ratio of 1/12 system. The result show the phase transformation of δ-, γ- and β-phase in the products sintered at 600–1000 °C for 3 h.

$$PbO_{(s)} + (5–6)Fe_2O_{3(s)} \rightarrow \beta\text{-phase}(PbO\cdot(5–6)Fe_2O_3)_{(s)} \quad (6)$$

The final products in the Pb/Fe of 1/12 system were β-phase along with some unreacted Fe_2O_3, similarly to the results described by Sahu et al. (2012). The β-phase was coexistent with some residue Fe_2O_3 in the system, this result may indicate that Pb/Fe molar ratio in the formed β-phase was more than 1/12. No phase change from solid to liquid was observed for the β-phase at 1000 °C; this result is consistent with the melting point of β-phase at 1265 °C, as determined by Chaudhury et al. (2008).

Further growth details of the β-phase and the reduction of Fe_2O_3 in Pb/Fe ratio of 1/12 system was shown in Fig. 3 (b) and (c). The highest peak of β-phase and Fe_2O_3 located at $2\theta = 32.28°$ and $2\theta = 33.17°$, which correspond to the (1 0 7) and (1 0 4) planes of their structures, respectively. The initial formation of crystalline β-phase was observed at 750–800 °C. Peak increase of β-phase at 800–950 °C indicated the continuing crystal growth of β-phase. The significant growth of the β-phase clearly occurred within the temperature range of 950–1000 °C. In contrast, a gradual decrease in the peak intensity of Fe_2O_3 was observed at the whole temperature range of 600–1000 °C. The results suggested the continuing incorporation of lead into lead ferrites by sintering PbO with Fe_2O_3.

3.4. The phase transformation mechanism analysis

As in the result in our previous section, the temperature for the effective formation of δ-phase and γ-phase was at around 800–850 °C, while the effective formation temperature of β-phase was at 950–1000 °C. Lead incorporation with Al_2O_3 and kaolin-based precursor was reported to be strongly dependent on the mass ratios of the Pb/Al and/or Pb/Si (Lu et al., 2013; Lu and Shih, 2015). Thus, the effect of Pb/Fe molar ratios was studied at temperatures of 800 and 950 °C for investigating the transformation mechanisms from lead to lead ferrites. When Pb/Fe was in the stoichiometric ratio of 1/1, δ-phase was observed to be the only Pb-hosting product at 800 °C (Fig. 4 (a)). As the Pb/Fe molar ratios decreased from 1/1 to 1/3, both δ-phase and γ-phase were observed as the main products. When the Pb/Fe molar ratio decreased from 1/4 to 1/7, γ-phase was still found to be the dominant product, but with a significant increase of β-phase and disappearance of δ-phase in the product. The influence of Pb/Fe molar ratios on phase transformation revealed that δ-phase was the dominate phase at Pb/Fe molar ratios of 1/1-1/3, but γ-phase was the favorable product at Fe-rich region (Pb/Fe molar ratios of 1/4-1/7) at 800 °C.

Two 2θ ranges of the XRD patterns ($2\theta = 31.9–33.1°$ and $31.4–32.0°$) were selected to further assess peak intensity changes with different Pb/Fe molar ratios (Fig. 4 (b) and (c)). The major peak of δ-phase quickly reached its maximum at Pb/Fe molar ratio of 1/1, and decreased with the reduction of Pb/Fe molar ratios. The peak intensity of γ-phase was weak in Pb/Fe molar ratios of 1/2-1/3 products, and the substantial formation of γ-phase was detected in Pb/Fe molar ratio of 1/4 product. This finding revealed a crystal growth of γ-phase with the decrease of Pb/Fe molar ratios from 1/2 to 1/4 and a gradual decrease with the reducing of Pb/Fe molar ratios from 1/4.5 to 1/7.

As shown in Fig. 5, the XRD patterns revealed the dominate formation of β-phase in sintered Fe-rich products. Small amount of γ-phase were observed at Pb/Fe molar ratios of 1/7 and 1/7.5. The conversion from γ-phase to β-phase was observed with the decrease of Pb/Fe molar ratios from 1/7.5 to 1/8. When Pb/Fe molar ratios ranged from 1/8 to 1/10.5, β-phase became the only product phase with chemical formula of $PbO\cdot(4–5.25)Fe_2O_3$. As mentioned in our previous section, the preference of residue Fe_2O_3 was found in the Fe-rich samples (Pb/Fe molar ratios of 1/11 to 1/12) because the chemical formula for the formed β-phase was not with Pb/Fe of

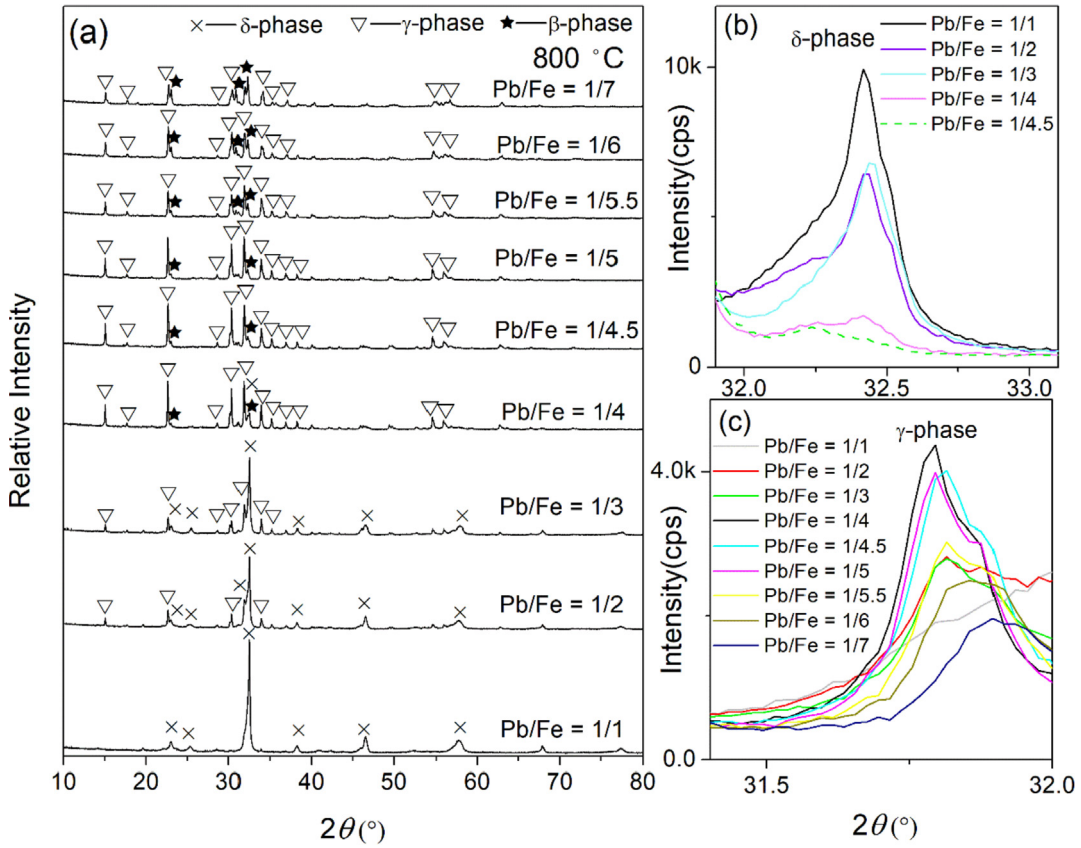

Fig. 4. XRD patterns for (a) $2\theta = 10–80°$, (b) $2\theta = 31.9–33.1°$ and (c) $2\theta = 31.4–32.0°$ of PbO/Fe_2O_3 system with different Pb/Fe molar ratios. The results show the changes in peak intensity of δ-, γ- and β-phase of the products sintered at 800 °C for 3 h.

1/12, but with Pb/Fe of 1/8 to 1/10.5. The formation of β-phase is demonstrated in more detail by the increase of the highest peak located at $2\theta = 32.28°$ (Fig. 5(b)). The increase of the diffraction peak demonstrated the continuing growth of β-phase with the increase of Fe_2O_3 content in the product. The presence of the residual Fe_2O_3 was found in the reaction systems with Pb/Fe molar ratios of 1/11-1/12 (Fig. 5(c)).

The reaction pathways for the formation of δ-, γ- and β-phase was illustrated in Fig. 6. At low temperatures of 700–800 °C, PbO/Fe_2O_3 systems with Pb/Fe molar ratios of 1/1-1/3 were dominated by the formation of δ-phase (pathway (I)). With the increase of temperatures to 750–850 °C and the reduction of Pb/Fe molar ratios from 1/4 to 1/7, the formation of γ-phase (pathway (II)) and the transformation of δ-phase to γ-phase (pathway (III)) were observed. At higher temperatures of 900–1000 °C, β-phase was considered as the dominant product at Pb/Fe molar ratios of 1/7-1/12. The formation of β-phase can be achieved by direct interaction between PbO and Fe_2O_3 (pathway (IV)), structure evolution from γ-phase to β-phase (pathway (V)), and the structure reconstruction from δ-phase to β-phase (pathway VI).

The chemical reactions process revealed the structure transformation among δ-phase, γ-phase and β-phase under different temperatures and Pb/Fe molar ratios. The δ-phase was reported with perovskite-based sub-lattice with space group of *I*4/*mmm* (Batuk et al., 2011). The Fe atoms are coordinated by the surrounding O atoms to form octahedral and tetragonal pyramids (Fig. 6). However, the structural arrangement of δ-phase is quite different from γ-phase and β-phase, which affords the opportunity for the reconstruction of the crystal structure during the formation of γ-phase and β-phase at higher temperatures and lower Pb/Fe molar ratios. The structural similarity of γ-phase and β-phase is likewise consistent with the fact that they share the same space group, $P6_3/mmc$ (Moore et al., 1989; Palomares-Sánchez et al., 2005). Thus, the transformation from γ-phase to β-phase suggested a structure evolution process. Following this structural evolution, local structural changes arose as a consequence of the addition of Fe_2O_3. With the decrease of Pb/Fe molar ratios from 1/4-1/10.5, the occupation of Fe in the defect Fe_2O_3 layers increased from 0.33 to 0.875 as γ-phase transformed to β-phase with chemical formula of $PbO·(4–5.25)Fe_2O_3$. (Fig. 6).

3.5. Leachability of the product phases

Because δ-phase, γ-phase and β-phase are potential lead ferrites in products with different PbO/Fe_2O_3 ratios, their lead leachability and leaching behavior need to be evaluated to optimize the lead stabilization strategy. Pure δ-phase ($PbO·Fe_2O_3$) was prepared from the sintered 1/2 Pb/Fe molar ratio PbO/Fe_2O_3 mixture at 750 °C for 3 h. The single γ-phase ($PbO·2Fe_2O_3$) was prepared by sintering the PbO/Fe_2O_3 mixture with Pb/Fe molar ratio of 1/4 at 800 °C for 12 h. The single β-phase ($PbO·5Fe_2O_3$) was obtained by sintering PbO/Fe_2O_3 mixture with Pb/Fe molar ratio of 1/10 at 1000 °C for 3 h. Fig. 7 shows the XRD patterns and the growth face (h k l) of lead ferrites (δ-, γ- and β-phase) used for the leaching test in this study.

A constant pH 4.9 leaching experiment was used to determine the Pb leachability in lead ferrites. The leachability of Pb in PbO was also used as a reference to compare with that of lead ferrites. Starting with a pH 4.9 leaching fluid, the lead concentration in the leachate of PbO was found to be as high as 16 g/L after only 0.5 h of leaching. Compared to lead ferrites, it was more than one hundred

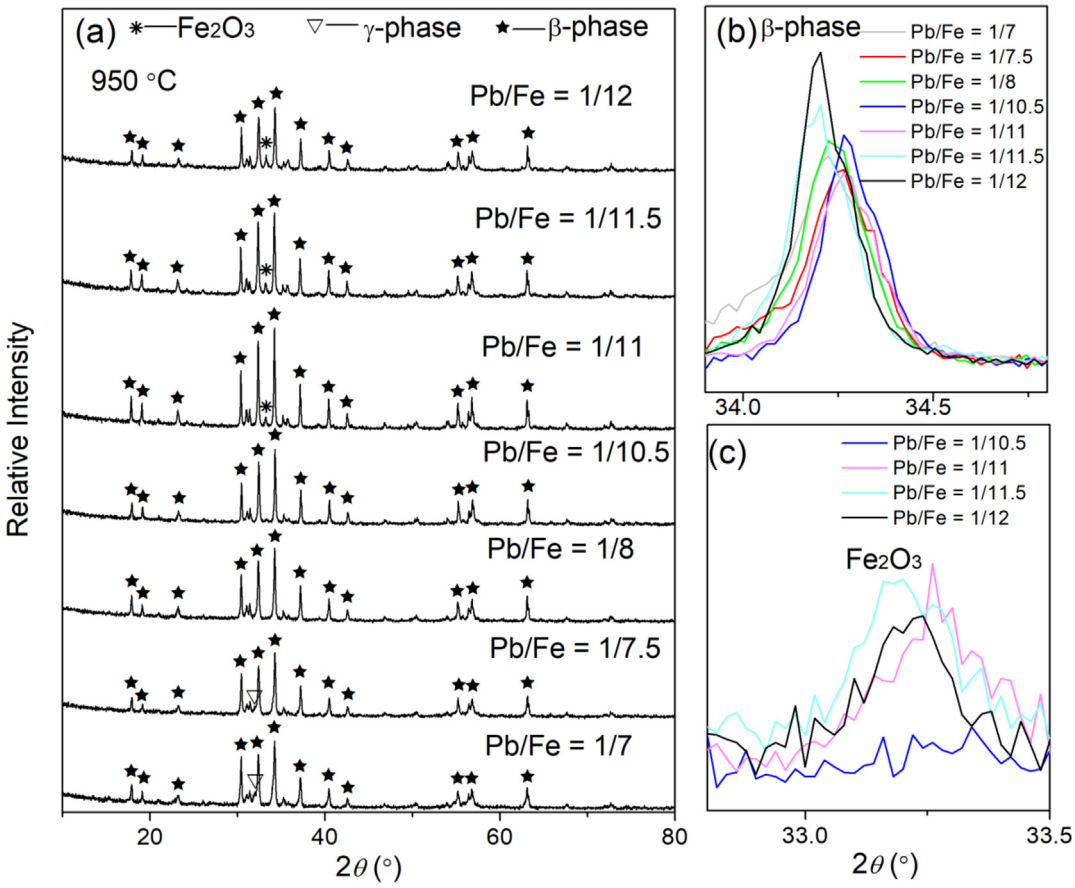

Fig. 5. XRD patterns for (a) $2\theta = 10–80°$, (b) $2\theta = 33.9–34.8°$ and (c) $2\theta = 32.8–33.5°$ of PbO/Fe_2O_3 systems with different Pb/Fe molar ratios. The results show the changes in peak intensity of the δ-, γ- and β-phase in the products sintered at 600–1000 °C for 3 h.

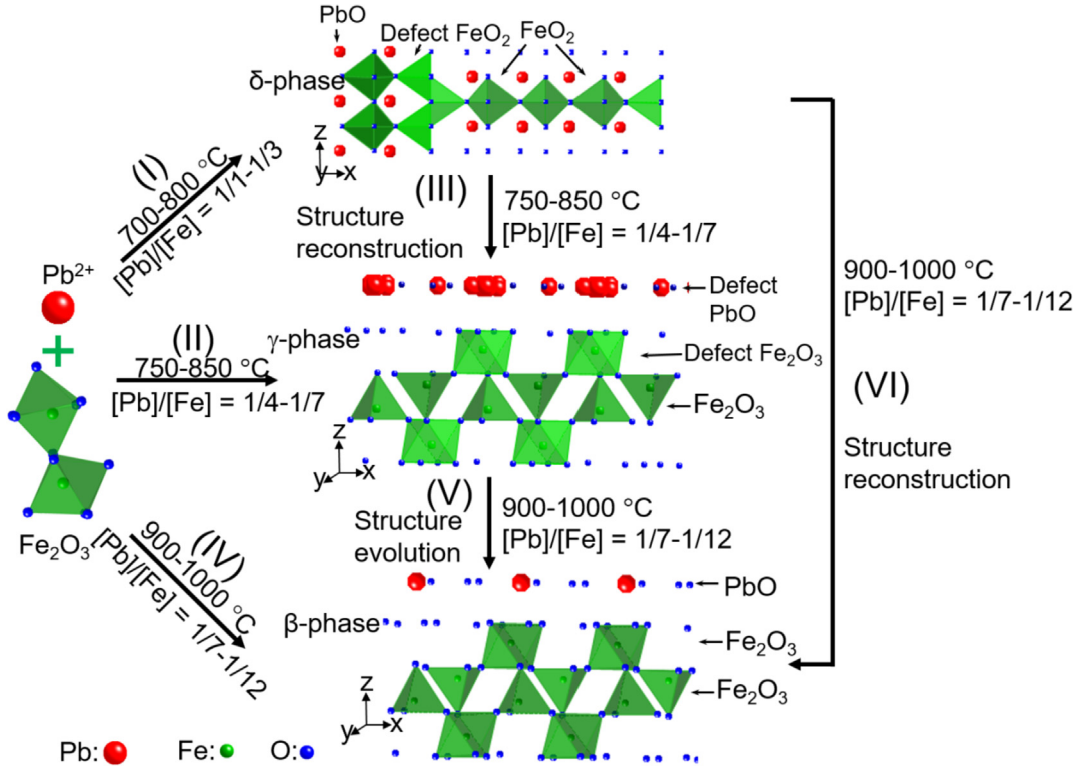

Fig. 6. Pathways for the formation of lead ferrites by sintering PbO and Fe_2O_3 at 600–1000 °C. Pathway (I) is the main reaction at 700–800 °C with Pb/Fe molar ratios of 1/1-1/3; pathways (II) and (III) are the main reaction at 750–850 °C with Pb/Fe molar ratios of 1/4-1/7; pathways (IV)-(VI) require higher temperatures of 900–1000 °C with lower Pb/Fe molar ratios of 1/7-1/12 to initiate.

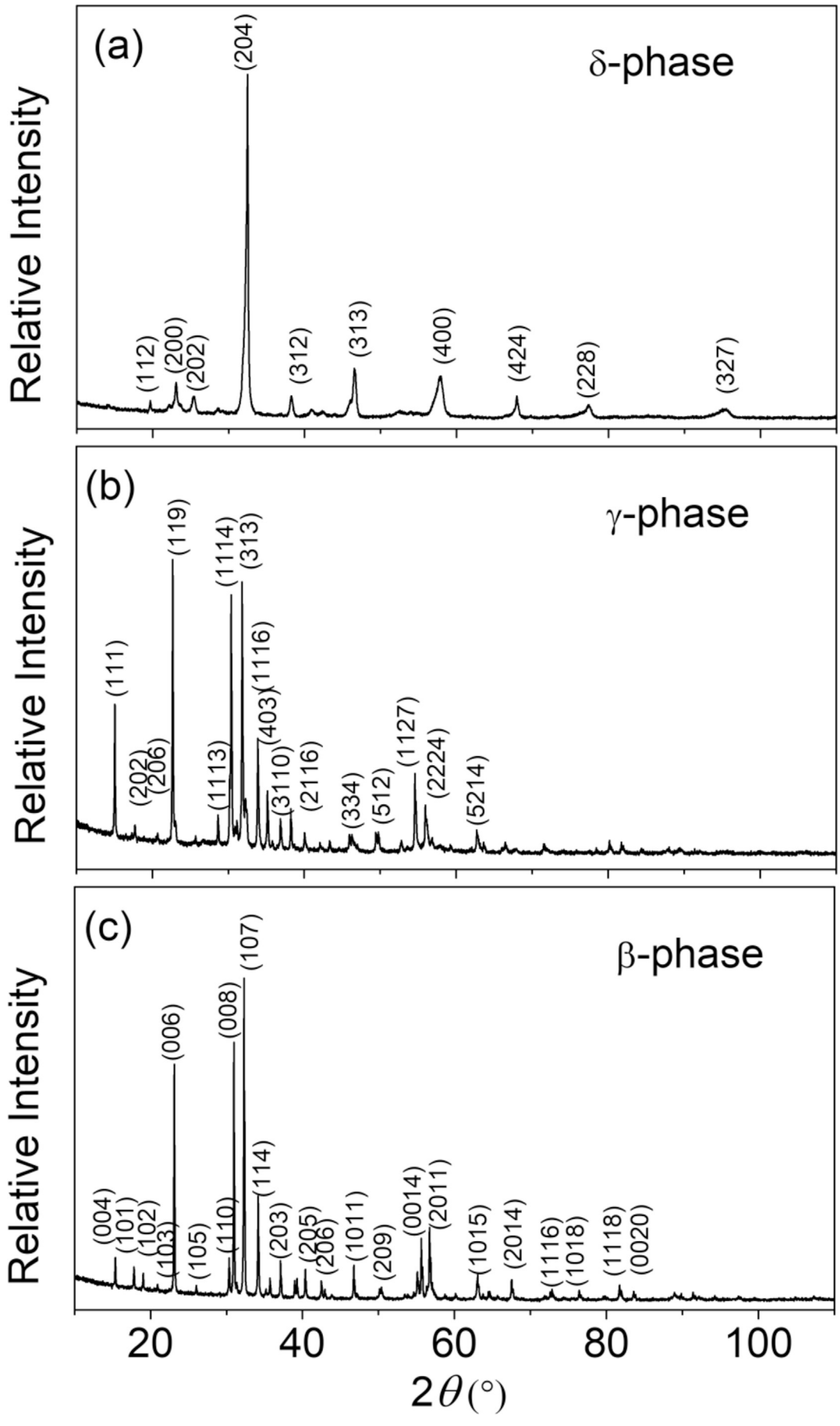

Fig. 7. XRD patterns and the growth face (h k l) of (a) δ-phase, (b) γ-phase and (c) β-phase generated in this study for leaching tests.

times higher than δ-phase (123 mg/L) and almost three orders of magnitude higher than γ-phase (21 mg/L) and β-phase (4 mg/L). The PbO was completely dissolved in the leaching fluid after 7 h, suggesting that the oxide form of lead is incapable of stabilizing lead under acidic conditions, and thus indicating that a strategy for transforming lead into a more robust hosting phase is needed.

To further understand the leaching behavior of lead ferrites, potential re-precipitation and surface modification regarding the Pb leachability were examined. At the end of the leaching period, The Pb concentration was found at around 249.9 mg/L (~$10^{-2.92}$ M) for the δ-, 25.6 mg/L (~$10^{-3.91}$ M) for the γ-, and 4.12 mg/L (~$10^{-4.70}$ M) for the β-phase leachate (Fig. 8(a)). The product of $[Pb^{2+}_{(aq)}] \times [OH^{-}_{(aq)}]^2$ in the δ-, γ- and β-phase leachate is thus $10^{-21.1}$, $10^{-22.1}$ and $10^{-22.9}$, which were all lower than the K_{spPb} ($10^{-14.92}$) (Al-degs et al., 2001) of $Pb(OH)_{2(s)}$. These results suggested that lead concentrations in the leachates of δ-, γ- and β-phase were all considerably under-saturated with respect to the $Pb(OH)_{2(s)}$ and the release of Pb should be controlled by the ferrite matrix.

Theoretically, if the δ-phase ($PbO \cdot Fe_2O_3$), γ-phase ($PbO \cdot 2Fe_2O_3$)

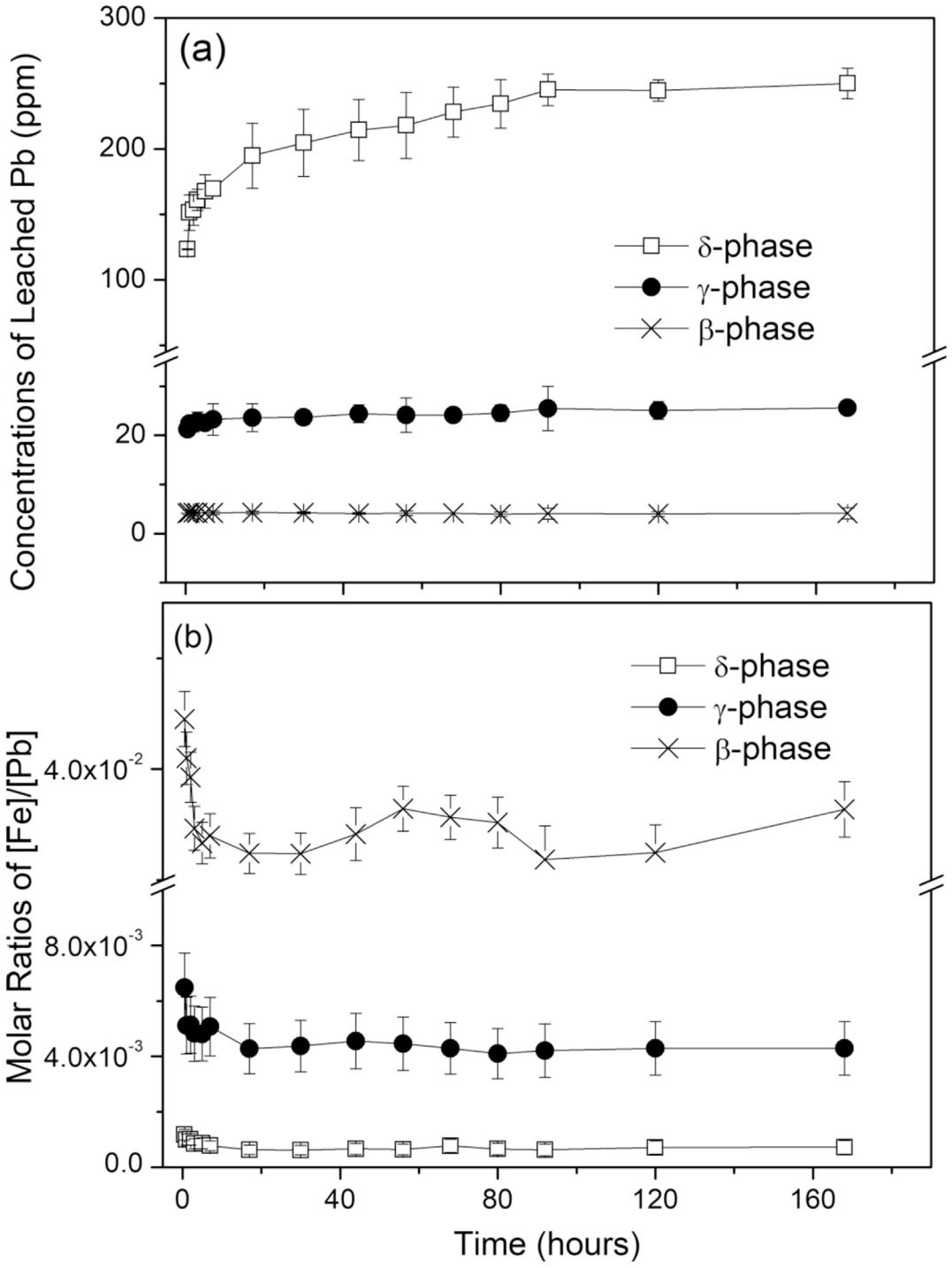

Fig. 8. Concentrations of leached Pb (a) and [Fe]/[Pb] molar ratios (b) from δ-phase, γ-phase and β-phase leachate.

and β-phase ($PbO \cdot 5Fe_2O_3$) solid displayed a congruent dissolution in the leaching process, the [Fe]/[Pb] molar ratios in the leachate would be at 2 for δ-phase, 4 for γ-phase and 10 for β-phase which is coincident with the stoichiometry of Pb and Fe ions in their original phase. However, the observed [Fe]/[Pb] molar ratios were all below the original stoichiometry of [Fe]/[Pb] in Fig. 8(b). The observed [Fe]/[Pb] ratio may indicate incongruent dissolution of δ-, γ- and β-phase ($PbO \cdot 5Fe_2O_3$) and/or the precipitation of ferric hydroxide in the leachates. The concentrations of [Fe^{3+}] may be limited by the potential precipitation/dissolution of the $Fe(OH)_{3(s)}$ (Stumm and Morgan, 1996):

$$Fe(OH)_{3(s)} \leftrightarrow Fe^{3+} + 3OH^- \ (K_{spFe} = 10^{-37.4}) \quad (7)$$

The iron ions in the solution may exist as different hydrolysis species depending on the pH value of the solution. At pH 5.0, the main species for iron ions are Fe^{3+}, $Fe(OH)^{2+}$, $Fe(OH)_2^+$, and $Fe(OH)_4^-$ (Stumm and Morgan, 1996). The hydrolysis process can be expressed as:

$$Fe^{3+} + H_2O \leftrightarrow FeOH^{2+}_{(aq)} + H^+ \left(K_{Fe1} = 10^{-2.2}\right) \quad (8)$$

$$Fe^{3+} + 2H_2O \leftrightarrow FeOH^{+}_{2\ (aq)} + 2H^+ \left(K_{Fe2} = 10^{-5.7}\right) \quad (9)$$

$$Fe^{3+} + 4H_2O \leftrightarrow FeOH^{-}_{4\ (aq)} + 4H^+ \left(K_{Fe4} = 10^{-21.6}\right) \quad (10)$$

Therefore, the total Fe ion concentration may be expressed as:

$$[Fe]_{total} \approx \left[Fe^{3+}\right] + \left[FeOH^{2+}\right] + \left[FeOH_2^+\right] + \left[FeOH_4^-\right] + 10^{4.1}\left[Fe^{3+}\right] \approx 5.58 \times 10^{-2} \text{mg/L}$$

The maximum Fe concentrations measured in the leachates of δ-, γ- and β-phase were about 4.8×10^{-2}, 4.12×10^{-2} and 4.9×10^{-2} mg/L, respectively. The measured Fe concentrations in the leachates did not reach the saturation of the estimated $[Fe]_{total}$. Therefore, neither Pb nor Fe ions were subject to reprecipitation from the leachates, and the observed [Fe]/[Pb] ratio may indicate a strong incongruent dissolution of δ-, γ- and β-phase in the leaching experiment, where the majority of the Fe-O bonds still remained on the surface of lead ferrites. This result suggested the accumulation of Fe-rich substance(s) on the surface of leached lead ferrites, which may also be beneficial for preventing further leaching of Pb from the lead ferrites. The overall result of leaching test demonstrated the feasibility of transforming lead bearing waste into lead ferrites, particularly into β-phase, to effectively reduce the geo-environmental hazard of metal waste.

4. Conclusions

The formation of δ-phase, γ-phase and β-phase was observed by sintering PbO with hematite at 600–1000 °C. At 700–800 °C, δ-phase was dominated in PbO/Fe_2O_3 system with [Pb]/[Fe] of 1/1-1/3. With the increase of temperatures to 750–850 °C, the significant formation of γ-phase was detected in Pb/Fe molar ratios of 1/4-1/7 products. The formation of β-phase can be initiated at 900–1000 °C with Pb/Fe molar ratios of 1/7-1/12. The structure reconstruction for transforming δ-phase to γ-phase and/or β-phase and structure evolution by conversing γ-phase into β-phase were detected in PbO/Fe_2O_3 system. As a comparison of the intrinsic properties of δ-phase, γ-phase and β-phase, the leaching experiment clearly illustrates the superiority of β-phase in stabilizing lead over longer leaching periods. The incorporation of lead-containing waste into lead ferric ceramic products by the formation of β-phase shows great promise.

Notes

The authors declare no competing financial interest.

Acknowledgments

This research was supported by Science and Technology Program of Guangzhou, China (201804010103), Shaoguan special fund for soil pollution and control (2017sgtyfz302), National Natural Science Foundation of China (Project 21637001), and the Research Fund Program of Guangdong Provincial Key Laboratory of Environmental Pollution Control and Remediation Technology (2018K18).

References

Al-Abed, S.R., Jegadeesan, G., Purandare, J., Allen, D., 2007. Arsenic release from iron rich mineral processing waste: influence of pH and redox potential. Chemosphere 66, 775–782.
Al-Degs, Y., Khraisheh, M.A.M., Tutunji, M.F., 2001. Sorption of lead ions on diatomite and manganese oxides modified diatomite. Water Res. 35 (15), 3724–3728.
Batuk, D., Hadermann, J., Abakumov, A., Vranken, T., Hardy, A., Van Bael, M., Van Tendeloo, G., 2011. Layered perovskite-like $Pb_2Fe_2O_5$ structure as a parent matrix for the nucleation and growth of crystallographic shear planes. Inorg. Chem. 50, 4978–4986.
Chaudhury, S., Rakshit, S.K., Parida, S.C., Singh, Z., Mudher, K.S., Venugopal, V., 2008. Studies on structural and thermo-chemical behavior of $MFe_{12}O_{19}$(s) (M= Sr, Ba and Pb) prepared by citrate–nitrate gel combustion method. J. Alloys Compd. 455, 25–30.
Conrad, K., Hansen, H.C.B., 2007. Sorption of zinc and lead on coir. Bioresour. Technol. 98 (1), 89–97.
Diop, I., David, N., Fiorani, J.M., Podor, R., Vilasi, M., 2010. Experimental investigations and thermodynamic description of the $PbO\text{-}Fe_2O_3$ system. Thermochim. Acta 510, 202–212.
Gupta, V.K., Agarwal, S., Saleh, T.A., 2011. Synthesis and characterization of alumina-coated carbon nanotubes and their application for lead removal. J. Hazard Mater. 185 (1), 17–23.
Hsieh, C.H., Shih, K., Hu, C.Y., Lo, S.L., Li, N.H., Cheng, Y.T., 2013. The effects of salinity and temperature on phase transformation of copper-laden sludge. J. Hazard Mater. 244, 501–506.
Hu, C.Y., Shih, K., Leckie, J.O., 2010. Formation of copper aluminate spinel and cuprous aluminate delafossite to thermally stabilize simulated copper-laden sludge. J. Hazard Mater. 181 (1–3), 399–404.
Islam, M.Z., Catalan, L.J., Yanful, E.K., 2004. Effect of remineralization on heavymetal leaching from cement-stabilized/solidified waste. Environ. Sci. Technol. 38, 1561–1568.
Jackson, D.R., Garrett, B.C., Bishop, T.A., 1984. Comparison of batch and column methods for assessing leachability of hazardous waste. Environ. Sci. Technol. 18, 668–673.
Li, M., Su, P., Guo, Y., Zhang, W., Mao, L., 2017. Effects of SiO_2, Al_2O_3 and Fe_2O_3 on leachability of Zn, Cu and Cr in ceramics incorporated with electroplating sludge. J. Environ. Chem. Eng. 5 (4), 3143–3150.
Li, N.H., Chen, Y.H., Hu, C.Y., Hsieh, C.H., Lo, S.L., 2011a. Stabilization of nickel-laden sludge by a high-temperature $NiCr_2O_4$ synthesis process. J. Hazard Mater. 198, 356–361.
Li, N.H., Lo, S.L., Hu, C.Y., Hsieh, C.H., Chen, C.L., 2011b. Stabilization and phase transformation of $CuFe_2O_4$ sintered from simulated copper-laden sludge. J. Hazard Mater. 190 (1–3), 597–603.
Lu, H.C., Chang, J.E., Shih, P.H., Chiang, L.C., 2008. Stabilization of copper sludge by high-temperature $CuFe_2O_4$ synthesis process. J. Hazard Mater. 150 (3), 504–509.
Lu, X., Shih, K., 2015. Formation of lead-aluminate ceramics: reaction mechanisms in immobilizing the simulated lead sludge. Chemosphere 138, 156–163.
Lu, X., Shih, K., Cheng, H., 2013. Lead glass-ceramics produced from the beneficial use of waterworks sludge. Water Res. 47 (3), 1353–1360.
Mao, L., Cui, H., An, H., Wang, B., Zhai, J., Zhao, Y., Li, Q., 2014. Stabilization of simulated lead sludge with iron sludge via formation of $PbFe_{12}O_{19}$ by thermal treatment. Chemosphere 117, 745–752.
Moore, P.B., Gupta, P.K.S., Le Page, Y., 1989. Magnetoplumbite, Pb(super 2+)Fe(super 3+) $_{12}O_{19}$; refinement and long-pair splitting. Am. Mineral. 74, 1186–1194.
Nevřiva, M., Fischer, K., 1986. Contribution to the binary phase diagram of the system $PbO\text{-}Fe_2O_3$. Mater. Res. Bull. 21, 1285–1290.
Palomares-Sánchez, S.A., Diaz-Castanon, S., Ponce-Castañeda, S., Mirabal-García, M., Leccabue, F., Watts, B.E., 2005. Use of the Rietveld refinement method for the preparation of pure lead hexaferrite. Mater. Lett. 59, 591–594.

Raghavan, V., 1989. In: Phase Diagram of Ternary Iron Alloys, Part 5, Ternary System Containing Iron and Oxygen. The Indian Institute of Metals, Calcutta, India.
Rivolier, J.L., Ferriol, M., Abraham, R., Cohen-Adad, M.T., 1993. Study of the PbO-Fe_2O_3 system. Eur. J. Solid State Inorg. Chem. 30, 727–739.
Sahu, S.K., Ganesan, R., Gnanasekaran, T., 2012. Studies on the phase diagram of Pb-Fe-O system and standard molar Gibbs energy of formation of '$PbFe_5O_{8.5}$'and $Pb_2Fe_2O_5$. J. Nucl. Mater. 426, 214–222.
Sahu, S.K., Ganesan, R., Gnanasekaran, T., 2013. The standard molar enthalpies of formation of $Pb_2Fe_2O_5$ (s) and $PbFe_5O_{8.5}$ (s) by acid solution calorimetry. J. Chem. Thermodyn. 56, 57–59.
Shih, K., White, T., Leckie, J.O., 2006. Nickel stabilization efficiency of aluminate and ferrite spinels and their leaching behavior. Environ. Sci. Technol. 40 (17), 5520–5526.
Stumm, W., Morgan, J., 1996. Inc. J. Aquatic Chemistry, 3rd ed. A Wiley-Interscience Publication, John Wiley and Sons.
Su, M., Liao, C., Chan, T., Shih, K., Xiao, T., Chen, D., Kong, L., Song, G., 2018. Incorporation of cadmium and nickel into ferrite spinel solid solution: X-ray diffraction and X-ray absorption fine structure analyses. Environ. Sci. Technol. 52 (2), 775–782.
Su, M., Liao, C., Lee, P.H., Li, H., Shih, K., 2017. Formation and leaching behavior of ferrite spinel for cadmium stabilization. Chem. Eng. Sci. 158, 287–293.
Tang, Y., Shih, K., Wang, Y., Chong, T.C., 2011. Zinc stabilization efficiency of aluminate spinel structure and its leaching behavior. Environ. Sci. Technol. 45 (24), 10544–10550.
Udayanga, W.C., Veksha, A., Giannis, A., Lisak, G., Chang, V.W.C., Lim, T.T., 2018. Fate and distribution of heavy metals during thermal processing of sewage sludge. Fuel 226, 721–744.
Venäläunen, S.H., 2011. Apatite ore mine tailings as an amendment for remediation of a lead-contaminated shooting range soil. Sci. Total Environ. 409, 4628–4634.
Xu, G.R., Zou, J.L., Li, G.B., 2008. Effect of sintering temperature on the characteristics of sludge ceramsite. J. Hazard Mater. 150, 394–400.
Xu, G.R., Zou, J.L., Li, G.B., 2009. Stabilization/solidification of heavy metals in sludge ceramsite and leachability affected by oxide substances. Environ. Sci. Technol. 43, 5902–5907.